Biochimica et Biophysica Acta, 942 (1988) 186–198
Elsevier

BBA 74058

Effects of basolateral ouabain, amphotericin B, cyanide and potassium on amiloride noise during voltage clamp of *Rana pipiens* skin support sodium-amiloride competition

T. Hoshiko, R.A. Grossman and Stefan Machlup

Department of Physiology and Biophysics, Department of Physics, Case Western Reserve University, Cleveland, OH (U.S.A.)

(Received 11 April 1988)

Key words: Sodium channel; Amiloride; Voltage clamp; Single-channel current; (*R. pipiens*)

In a previous study, the amiloride-induced corner frequency (f_c) was found to decrease as apical sodium was increased. This effect was small or absent when the basolateral surface was exposed to high potassium. It has been suggested that the apical sodium effect may be indirect, due either to increased intracellular [Na^+] which repelled amiloride or to an increased potential at the apical surface which reduced amiloride affinity. High basolateral K^+ might then suppress the sodium effect either by preventing intracellular [Na^+] from increasing or by allowing a better clamp of the apical membrane potential by reducing basolateral membrane resistance and potential. We checked the effects of basolateral [K^+], of cyanide and of ouabain at concentrations known to increase intracellular [Na^+]. We found only negligible effects on f_c. In addition, amphotericin B added to the basolateral bathing solution either in 115 mM Na^+ or in 120 mM K^+ had no significant effect on f_c. We found that relatively wide variation in clamp potential under all conditions, even with active transport severely inhibited, left f_c virtually constant. Since the amiloride kinetics were independent of clamp potential, we were able to measure paracellular and transcellular conductances separately by examining the voltage dependence of clamp current (linear) and amiloride noise power (quadratic). This made possible estimation of channel density and single-channel current.

Introduction

In a previous study [1,2], a direct competition between sodium and amiloride for a common site was suggested. In that study, the characteristic spectral frequencies of triamterene- and amiloride-induced fluctuations in frog skin were found to decrease with increasing sodium concentration $[Na]_a$ in the apical bathing solution. This effect cannot be accounted for by the sodium self-inhibition mechanism of the three-state model of Lindemann and Van Driessche [3]. In their model, increasing apical sodium concentration increases the corner frequency, contrary to what we found. We therefore proposed a different model for competition between sodium and blocker [4].

In 1979, Van Driessche and Lindemann [5] reported the amiloride corner frequency to be independent of apical sodium concentration. Their experiments had been carried out in frog skins in which the basolateral surface was depolarized by a high potassium concentration. The rationale was to eliminate the possibility that the impedance of

Correspondence: T. Hoshiko, Department of Physiology and Biophysics, School of Medicine, Case Western Reserve University, 2119 Abington Road, Cleveland, OH 44106, U.S.A.

the basolateral membrane in series with an apical noise source might distort the spectrum (cf., Van Driessche and Gögelein [6], and Lindemann and DeFelice [7]). Hoshiko and Van Driessche [2] verified that the amiloride corner frequency becomes virtually independent of $[Na^+]_a$ when Na in the basolateral bathing solution is replaced with K^+. The fact that basolateral potassium could eliminate or minimize the sodium effect at the apical surface led to three hypotheses to explain the sodium effect as an indirect consequence of the presence of the basolateral membrane.

First, the use of a normally polarized epithelium may have distorted the spectral data. This possibility has been rejected since at high $[Na^+]_a$, the amiloride corner frequency is unaffected by replacement of basolateral sodium with potassium. The second hypothesis is that the presence of high $[Na^+]$ in both apical and basolateral solutions can increase intracellular $[Na^+]$, which may then repel amiloride binding. Sodium accumulation is prevented by incubation in potassium [8]. Increased intracellular $[Na^+]$ has been reported to increase the amiloride inhibition constant [9]. On the other hand, Cuthbert and Shum [10] state that ouabain did not change amiloride affinity in *Rana temporaria* skin. However, the radioligand binding method grossly overestimates channel density, and this result could not be considered definitive. A third hypothesis was offered by Lindemann [11], that the effect may result because increased apical sodium gradient causes an increased apical membrane potential [12] and that the on-rate constant for amiloride association with a membrane site is voltage-dependent. This sequence of events would be avoided by depolarization of the basolateral membrane with high $[K^+]$. If either intracellular sodium or voltage sensitivity of amiloride kinetics were the proximate cause of the effect on amiloride corner frequency then a direct sodium-amiloride competition at the apical channel need not be invoked.

In this study, we examine the effects on amiloride corner frequency of conditions which test these three hypotheses. We used conditions which (1) reduce basolateral membrane potential and resistance; (2) increase intracellular sodium by inhibiting active transport at levels known to increase intracellular sodium; and (3) alter apical membrane potential by clamping the skin at $\pm$ 50 mV. We show that amiloride corner frequency remains unchanged (1) after treatment of the basolateral surface with potassium; (2) after inhibition of active transport with ouabain at concentrations known to increase intracellular $[Na^+]$ [13] or with cyanide; and (3) that the amiloride corner frequency is virtually independent of clamp potential over the range of potentials that could reasonably be expected under the conditions of our original observations [2]. Thus, the sodium effect cannot be accounted for by indirect effects (1) as an artifact due to distortion, (2) as due to increased intracellular $[Na^+]$, or (3) as due to increased apical membrane voltage. We conclude that a direct interaction of sodium with amiloride is indeed the mechanism for the sodium effect.

Having observed that the amiloride corner frequency is virtually independent of clamp potential over the physiological range of potentials, we were able to analyze the effects of clamp voltage on noise power. We have found it possible to estimate separately the conductances of the transcellular and the paracellular pathways. In some epithelia, paracellular resistance has been reported to be increased by blocker [14], but it is unlikely that such non-specific blocking action could give rise to current fluctuations as they do at blocker-specific, ion-selective channels. The analysis supports the internal consistency of the application of noise analysis to amiloride-induced fluctuations, and is consistent with the epithelial noise equivalent circuit [15] derived from Ussing and Zerahn's electrical equivalent circuit of frog skin and its extension [16–18].

The purpose of this work was to test the above hypotheses for explaining the apical sodium effect as an indirect effect, hypotheses made plausible by the fact that basolateral potassium mitigates the sodium effect. Although the present experiments refute these hypotheses, they do not explain the mechanism of the basolateral potassium effect.

Preliminary reports of portions of this work were made at the Annual meetings of the Biophysical Society in 1984 [32] and 1987 [44].

Methods

Abdominal skins of *Rana pipiens* were mounted in a Helman-type chamber [19] as previously described [2]. The exposed area ranged from 0.28 to 0.79 cm^2. 3 M KCl-agar bridges and sintered Ag-AgCl electrodes were used in a 4-electrode voltage clamp [20]. The primary solution used was (in mequiv./l): 115 Na, 5 K, 1 Ca, 5 Tris (pH 7.8) with sulfate as the anion. For the high potassium solution, sodium was replaced with potassium. Solutions were changed frequently using a syringe, obviating need for continuous aeration. Amiloride was a gift from Merck, Sharp & Dohme, West Point, PA. Cyanide (5 mM KCN) and ouabain (0.1 mM, Nutritional Biochemicals) were used to inhibit active transport.

Amphotericin B (Squibb-Fungizone) was diluted to a final concentration of 10 μg/ml in the solution bathing the basolateral surface. Amphotericin B was used to prevent basolateral conductance from decreasing in the presence of inhibitors [21].

The amiloride-induced fluctuations are assumed to reflect specific blockage of sodium-selective apical channels [11]. Current fluctuations were induced by 2 μM amiloride in $[Na^+] = 115$ mequiv./l in the apical bathing solution and analyzed with a spectrum analyzer (Federal Scientific/Nicolet UA-500). Amiloride at 2 μM gives corner frequencies of about 3–5 Hz, whereas at higher concentrations, sodium current becomes progressively blocked and amiloride-induced fluctuations are buried in the background residual noise (cf. Refs. 2 and 4). Spectra with corner frequencies below 1 Hz are dominated by sodium noise.

Usually 32 individual power spectra (500 points each) were averaged using a PDP 11/24 computer. The 500 points were reduced to 90 points by averaging over frequency to obtain more even spacing on a logarithmic scale. Spectra were fitted as a Lorentzian function plus a $1/f$ component using a nonlinear least-squares procedure of Van Driessche and Zeiske [22]. The Lorentz spectral parameters (i.e., the low-frequency plateau S_o and the corner frequency f_c) were stable over considerable periods of time, allowing successive experimental manipulations. In addition to the standard initial condition, in which the basolateral solution was 115 mM Na^+, the experimental conditions (all of which involved the basolateral solution) were as follows: high basolateral potassium $[K^+]_i = 120$ mM; 10 μg/ml amphotericin B; 5 mM KCN; and 0.1 mM ouabain. All solutions contained 0.5 mM Ca^{2+}. For each condition, the clamp voltage was altered by 10 mV steps starting at 0 mV and going to +50 mV and to −50 mV, with the basolateral solution taken as the reference. In each experimental solution, spectra were averaged from up to 14 voltage clamps except following inhibitor treatment. The effects of experimental solutions were assessed by making paired comparisons at equivalent clamp voltages. For each comparison, data were obtained from at least four and usually five frog skins. Student's t-test was used to report significant differences ($P < 0.05$).

Instead of reporting the currents and plateau values at each clamp voltage for each experimental condition, we report the average coefficients relating the currents and plateaus to clamp voltage in the presence of 2 μM amiloride. From these values it is possible to obtain the short-circuit (zero clamp potential) values of current and plateau as well as the open-circuit (i.e., zero-current) values of potential and plateau.

Results

The effects of the experimental conditions on the amiloride corner frequency are considered first, and then the effects of clamp voltage on amiloride corner frequency are described. Finally, the effects of clamp voltage on noise power (plateau value) are described.

1. Effect on f_c

(a) Basolateral $[Na^+]_i$ vs. $[K^+]_i$

The plateau (S_o) was usually decreased in $[K^+]_i$ compared to that in $[Na^+]_i$, as shown in Fig. 1 (upper curve (+) in 115 Na vs. middle curve (□) in 120 K). This is not surprising since current was depressed with high $[K^+]_i$. However, as summarized in Table I, line 1, the amiloride corner frequency f_c was unchanged.

(b) Effect on f_c of 10 μg/ml amphotericin B

Amiloride spectra were virtually unchanged in

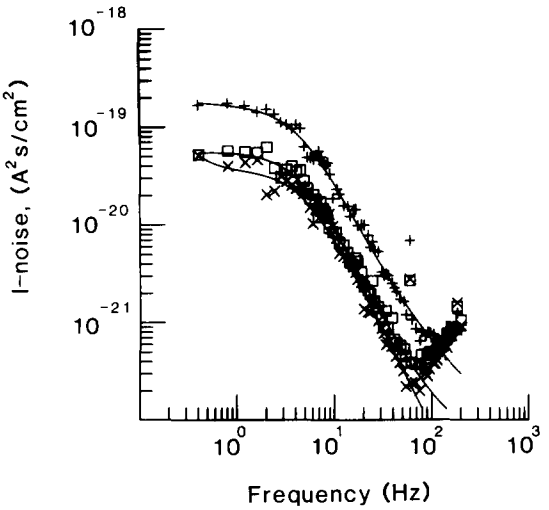

Fig. 1. Amiloride spectra from a skin clamped at 0 mV, (a) in basolateral $[Na]_i = 115$ mM, $[K]_i = 5$ mM, upper curve (+); (b) in $[K]_i = 120$ mM, middle curve (□); and (c) in $[K]_i = 120$ mM and 0.1% amphotericin B, lower curve (×). The corner frequencies were 4.2, 4.3, and 4.9 Hz, respectively. The plateau (S_o) was usually decreased in $[K]_i$ compared to that in $[Na]_i$, but the corner frequency was unchanged. After addition of amphotericin B to Na^+-free, high K^+ basolateral solution ((b) vs. (c)), the corner frequency showed a small increase which was not significant.

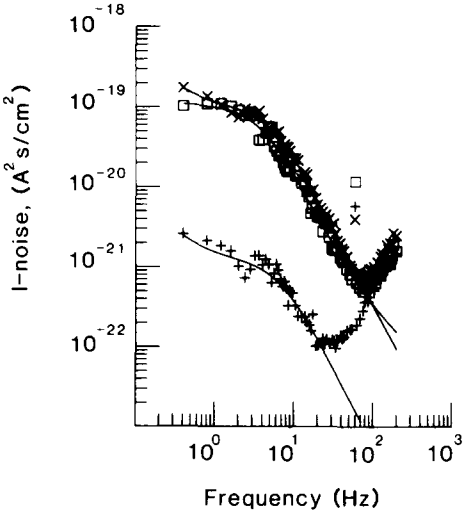

Fig. 2. Amiloride spectra from a skin clamped at 0 mV, in basolateral $[Na]_i = 115$ mM, $[K]_i = 5$ mM. (a) Control, middle curve (□); (b) 0.1% amphotericin B, upper curve (×); and (c) 0.1% amphotericin B plus 0.1 mM ouabain, lower curve (+). The corner frequencies were 3.9, 5.3, and 6.6 Hz, respectively in this skin. Amphotericin B did not change f_c or the plateau significantly when added to high Na basolateral solution ((a) vs. (b)). Ouabain in high Na^+ basolateral solution inhibited short-circuit current (16 to 0.7 $\mu A/cm^2$) and plateau, but its effect on f_c was not significant ((b) vs. (c)).

skins bathed in $[Na^+]_i = 115$ and $[K^+]_i = 5$ mequiv./l when amphotericin B was added to the basolateral solution. (Fig. 2, control (□) vs. amphotericin B (×) and summarized in Table I, line 2). In skins bathed in Na^+-free high-K^+ basolateral solution, the corner frequency showed

TABLE I

EFFECTS OF BASOLATERAL K^+, AMPHOTERICIN B, CYANIDE AND OUABAIN ON AMILORIDE (2 μM) CORNER FREQUENCY (PAIRED COMPARISONS)

Conditions compared I vs. II	Corner frequency (Hz) mean value I	II	mean diff. II − I	S.E. mean diff.	d.f.	t
$[Na]_i$ vs. $[K]_i$	4.27	4.02	−0.25	0.18	55	1.39
Control vs. amphotericin B $[Na]_i = 115$; $[K]_i = 5$	4.63	4.65	0.014	0.10	49	0.14
Control vs. amphotericin B $[Na]_i = 0$; $[K]_i = 120$	3.87	4.09	0.22	0.12	51	1.87
Control vs. 5 mM CN $[Na]_i = 0$; $[K]_i = 120$	3.93	4.13	0.20	0.15	35	1.36
Control vs. 0.1 mM ouabain $[Na]_i = 115$; $[K]_i = 5$	4.55	4.27	−0.38	0.16	38	1.73
Control vs. 0.1 mM ouabain $[Na]_i = 0$; $[K]_i = 120$	5.24	4.78	−0.46	0.18	33	2.58 **

** $P < 0.025$.

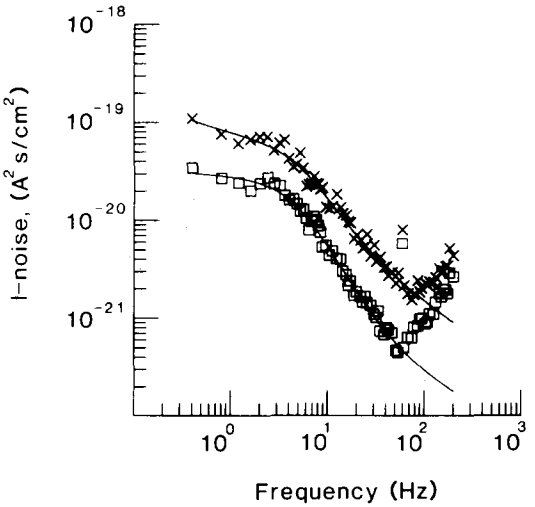

Fig. 3. Amiloride spectra from a skin clamped at 0 mV, in basolateral $[K]_i = 120$ mM and 0.1% amphotericin B. (a) Control, upper curve (×), and (b) plus 5 mM KCN, lower curve (□). The corner frequencies were 5.0, and 4.7 Hz, respectively this experiment. Cyanide depressed both short-circuit current (from 13 to 5 $\mu A/cm^2$) and plateau but left the corner frequency unchanged for the series.

a small increase which was not significant upon basolateral addition of amphotericin B (Fig. 1, control (□) vs. amphotericin B (+) and Table I, line 3). The clamp current in amiloride was unchanged by amphotericin B as indicated by a paired comparison *t*-test of 49 periods in four skins (data not shown).

(c) Effect on f_c of 5 mM cyanide

Addition of cyanide to the basolateral solution led to a prompt fall in short-circuit current I_{sc} over 30 minutes to less than a quarter of the initial value. The plateau values were decreased but the corner frequency change was not significant (Fig. 3, control (×) vs. cyanide (□) and Table I, line 4).

(d) Effect of 0.1 mM ouabain

The basolateral surface was exposed to 0.1 mM ouabain in 115 Na^+, 5 K^+ sulfate Ringer's and amphotericin B. Over the course of 45 to 60 min, I_{sc} was inhibited to less than 10% and in some cases resulted in negative values even though both surfaces were bathed in identical solutions except for the ouabain. After one hour of exposure to ouabain, amiloride current spectra were obtained. The plateau was depressed to less than 20% of its initial value and the corner frequency was slightly decreased, but not significantly (Fig. 2, control (□) vs. ouabain-treated (+) and Table I, line 5). Lorentzian spectra were obtained even with negative clamp currents, a finding also reported by Van Driessche and Erlij [23] but under different conditions.

When the basolateral surface was exposed to 120 K^+ sulfate Ringer's containing ouabain and amphotericin B, I_{sc} was inhibited to less than 20% of the initial value. Then upon exposure to amiloride, the plateau was inhibited to about 30% of its value before ouabain. The corner frequency decreased by a small amount, which was significant (Table I, line 6). These experiments with ouabain and basolateral potassium were carried out with a somewhat different protocol than the other experiments. Instead of stepping the clamp voltages up and then down, the polarity at each voltage level was applied in succession, i.e., +10 then −10, etc. The protocol was altered in later experiments since the time for the current to settle after large voltage steps was rather long.

2. Effect of clamp voltage on corner frequency

As described in Methods, the clamp voltage was varied form +50 to −50 mV in 10 mV steps and amiloride spectra were obtained at each clamp level. At the beginning and end of each series, a spectrum was taken at 0 mV. In some cases, duplicate spectra were obtained as well. After inhibition of transport by ouabain or by cyanide, the currents in amiloride were so low or even negative, especially at the negative, hyperpolarizing potentials, that spectra were rarely obtainable at potentials more negative than −20 mV. A total of 705 spectra were obtained in 59 conditions using 24 frogs. One experiment consisted of only five spectra and was eliminated from further analysis. Thus f_c-voltage curves in the 58 experiments averaged about 12 spectra per curve and ranged from 6 to 19 spectra. For each curve, a stepwise polynomial regression was carried out in order to determine whether an additional square term in voltage improved the fit, i.e., to test the linearity of the fit [24]. Out of the 58 curves five showed the square term to be significant at the 2.5% level and an additional two at 5%. The mean values of the

ordinate intercept and of the slope were 4.48 Hz and +0.0069 Hz/mV, respectively. Of the 58 slopes, 45 were positive and 13 were negative. Although the mean slope was significantly different from zero ($P < 0.01$), the slope was quite small and equalled less than 15% of the corner frequency over a 100 mV range of clamp voltage. This cannot account for the 2- and 3-fold changes in f_c with sodium [2].

Palmer [25,26] and Warncke and Lindemann [27,28] reported that in toad bladder, amiloride inhibition was voltage sensitive. The effect was discernable only at the higher concentrations of the blocking agent or at large clamp voltages. This is evident in Fig. 2 or Warncke and Lindemann [27]. Their studies are consistent with our previous [1,2] as well as the present study that over the range of −50 to +50 mV, and amiloride concentration under 1.8 μM the voltage effect is negligible. However, both Palmer and Warncke and Lindemann used high serosal potassium, a condition which greatly mitigates the apical sodium effect.

3. Effect of clamp voltage on plateau and clamp current

Both the plateau (S_o) and clamp current (I) increased with increased clamp voltage (V). The current-voltage (I-V) relationships were linear (see Fig. 4a) with only 8 out of 58 slopes showing significant curvature ($P < 0.05$). One experiment was omitted from further analysis because total skin resistance was very low.

The effects on noise power were analyzed assuming that current flows across the frog skin via an intracellular route through apical channels and via an extracellular shunt pathway through tight junctions. First of all, since S_o is proportional to the square of the single-channel current, we would expect S_o to be proportional to the square of the amiloride-blockable channel current [15]. Since channel current is linearly related to voltage, S_o should be related to the square of the clamp voltage. It turns out (see Appendix) that S_o is predicted to be a quadratic function both of clamp current and of voltage:

$$S_o = A_0 + A_1 \cdot V + A_2 \cdot V^2$$

Of the 57 "A_2" coefficients representing curvature, in 16 cases inclusion of the A_2 coefficient reduced the variance significantly at 1% and a total of 27 were significant at 5%. In the same way, S_o was fitted as a quadratic function of I, yielding another set of three coefficients B_0, B_1, and B_2, of which 18 were significant at 1% and 31 at 5%. Sample plots are shown in Figs. 4b and 4c.

TABLE II

DEPENDENCE OF PLATEAU ON CURRENT AND VOLTAGE

Experiment	n	S_o vs. V_{clamp} ($\times 10^{20}$)			S_o vs. I_{clamp} ($\times 10^{20}$)			I vs. V	
		A_0	A_1	A_2	B_0	B_1	B_2	C_0	C_1
$[Na]_i = 115$ mM	9	11.8	0.275	0.0019	5.00	0.899	0.069	5.34	0.18
$[Na]_i = 115$ mM, amphotericin B	4	11.3	0.262	0.0017	4.78	0.770	0.043	6.18	0.21
$[Na]_i = 115$ mM, amphotericin B, 0.1 mM ouabain	3	1.34	0.061	0.0010	1.19	0.567	0.086	0.20	0.12
$[K]_i = 120$ mM	4	9.75	0.403	0.0050	4.89	0.829	0.052	3.68	0.28
$[K]_i = 120$ mM, amphotericin B	11	14.2	0.533	0.0069	5.25	0.785	0.047	7.40	0.46
$[K]_i = 120$ mM, amphotericin B, 5 mM CN	3	4.33	0.288	0.0026	1.57	0.579	0.065	1.91	0.25
$[K]_i = 120$ mM, amphotericin B, 0.1 mM ouabain	4	2.99	0.212	0.0044	1.48	0.159	0.021	2.10	0.57

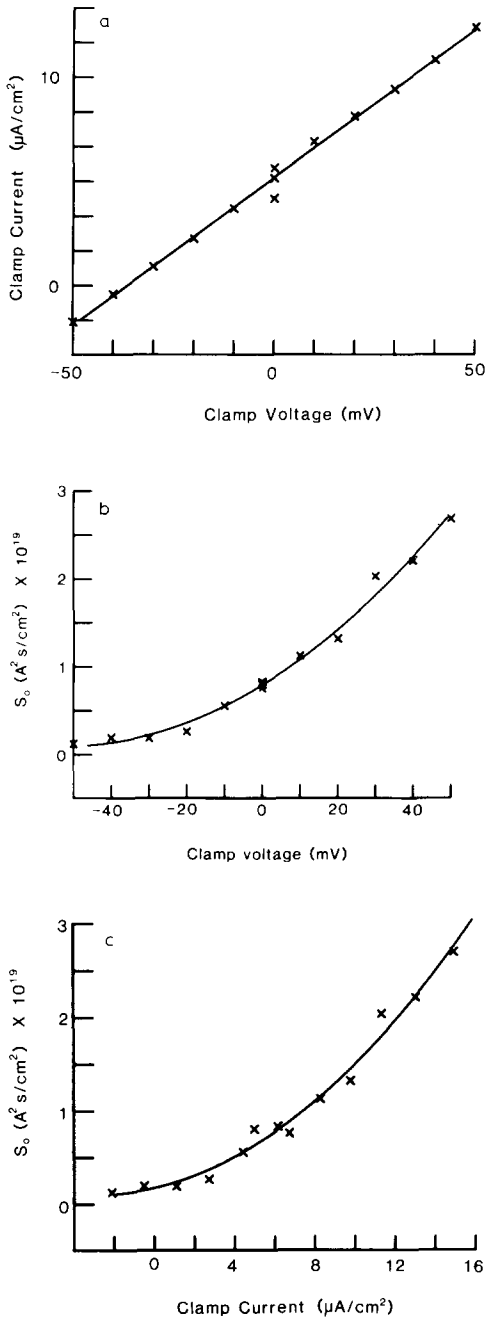

Fig. 4. (a) Representative current-voltage plot, showing experimental points and fitted straight line: $I = C_0 + C_1 \cdot V$. (b) representative plot of plateau (S_o) versus the clamp voltage, V. A quadratic function was fitted to estimate the A-parameters: $S_o = A_0 + A_1 \cdot V + A_2 \cdot V^2$. (c) Representative plot of plateau (S_o) versus the clamp current, I. A quadratic function was fitted to estimate the B-parameters:

$$S_o = B_0 + B_1 \cdot I + B_2 \cdot I^2.$$

The three A coefficients must be positive and obey the relationship

$$4\,(A_0 A_2)/(A_1)^2 = 1$$

Analogous restrictions hold for the 'B' coefficients. Of the 57 experiments, 15 experiments had negative A_2 or B_2 coefficients and were eliminated from further analysis. An additional four experiments with ratios larger than 100 or smaller than 0.01 were not used in subsequent calculations. Average values of 'A' and 'B', together with the slopes C_1 (total conductance) and current intercepts C_2 (short-circuit current) for the remaining 38 current-voltage curves, are listed in Table II for the seven control and experimental conditions.

The six 'A' and 'B' parameters were interpreted in terms of the membrane emf E in the cellular pathway, a coefficient k relating the plateau to the square of the mean single-channel current, a coefficient c relating the short-circuit current to the single-channel current, and the transcellular and shunt pathway conductances g_o and g_s, respectively. From these considerations, it is possible to estimate g_s in three possible ways, the sum $(g_s + g_o)$ in four ways and E in nine. A simple average was taken for the conductance estimates; the median was used for estimating E.

The total conductance, which is the sum of the cellular and shunt pathway conductances, compared rather closely with the conductance $(g_s + g_o)$ obtained as the slope of the steady-state current-voltage curve for the same set of experiments. A paired comparison t-test failed to show a significant difference (Table III, line 1). The paired estimates are plotted against each other in Fig. 5a together with the 45-degree equality line rather than the linear fit, whose ordinate intercept and slope were -0.085 (± 0.06) mS/cm^2 and 1.51 (± 0.14), respectively. The linear correlation coefficient was 0.87. The current intercept of the I-V curve should be equal to $(E \cdot g_o)$ calculated from the values as estimated from the noise data. The paired comparison t-test showed no significant difference (Table III, line 2). These estimates are also plotted against each other in Fig. 5b together with the 45-degree equality line rather than the linear fit, whose ordinate intercept and slope were -0.98 (± 0.84) μA/cm^2 and 1.15 (± 0.12), respec-

TABLE III

COMPARISON OF SLOPE $(g_o + g_s)$, SHORT-CIRCUIT CURRENT $(E \cdot g_o)$ AND OPEN-CIRCUIT POTENTIAL $(E \cdot g_o)/(g_o + g_s)$, FROM *I-V* CURVE WITH VALUES CALCULATED FROM S_o DATA

Parameter	From *I-V*	From S_o	Mean diff.	S.E. diff.	d.f.	*t*
$(g_o + g_s)$ $(mS \cdot cm^{-2})$	0.317	0.393	0.076	0.043	37	1.77
$(E \cdot g_o)$ $(mA \cdot cm^{-2})$	4.83	4.50	−0.25	0.61	37	0.41
$\frac{(E \cdot g_o)}{(g_o + g_s)}$ (mV)	17.2	16.3	−0.96	1.08	37	0.89

tively. The slope is not significantly different from unity. The linear correlation coefficient was 0.84. Note that the quantity $E \cdot g_o$ (the ordinate intercept) is the zero-voltage current, while the ratio $E \cdot g_o/(g_o + g_s)$ or voltage intercept is the zero-current potential, both determined in the presence of amiloride. The zero-current potentials were calculated for each experiment from the *I-V* curve and from the noise data. The two estimates were plotted against each other (not shown) and fitted with a straight line, giving ordinate intercept, slope and linear correlation coefficient of -0.93 (± 1.7) mV, 1.00 (± 0.08), and 0.91, respectively. Again the paired comparison *t*-test showed no significant difference (Table III, line 3).

Discussion

From our results, we conclude that amiloride-induced spectra are not significantly distorted by the electrical properties of the basolateral membrane under the conditions used. Li et al. [29] in six skins of *Rana ridibunda* and Tang et al. [30] in eight skins of *R. pipiens* determined the amiloride on-rate constant before and after K^+-depolarization and found no significant change. The use of Na^+-free, high-K^+ basolateral solution [31] to circumvent possible distortion of amiloride-induced noise appears unnecessary. The presence of a normal basolateral emf does not significantly distort amiloride-induced fluctuations at the apical surface. The fact that all manipulations affecting active transport of basolateral membrane potential and/or resistance leave the amiloride corner frequency unchanged reaffirms that amiloride-induced fluctuations arise at the apical surface.

Thus the original demonstration of the apical sodium effect is not an artifact arising from the use of normally polarized skins. Actually, high basolateral K^+ may introduce additional complexities. When amphotericin B was used in addition to high potassium in the basolateral solution, a small effect on the amiloride corner frequency was noticed, which just failed to reach statistical significance. Although unaffected by ouabain in the presence of basolateral Na^+, the corner frequency

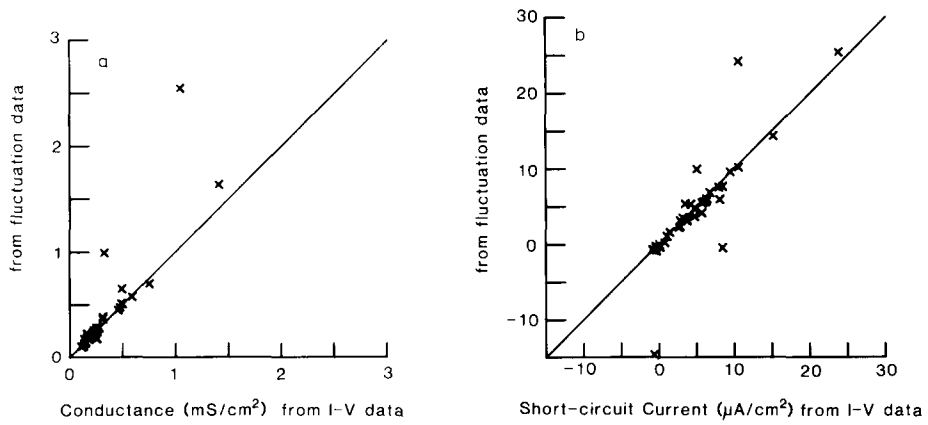

Fig. 5. (a) Total skin conductance estimated from fluctuation data plotted against conductance obtained as slope of the *I-V* curve. (b) Short-circuit current estimated from fluctuation data $(E \cdot g_o)$ plotted against I_{sc} obtained as the intercept of the *I-V* curve on the current axis.

did show a small but significant increase in the presence of high basolateral K^+. These results indicate that high basolateral K^+ may have effects on more than simply the electrical properties of the basolateral membrane, a suggestion made previously [32].

Our second conclusion is that the sodium effect is not attributable to a secondary effect of increased intracellular sodium. We applied the inhibitors CN and ouabain in concentrations which greatly depressed the short-circuit current. Intracellular sodium was shown to increase 9-fold after ouabain by Rick, et al. [13] in *Rana temporaria* and *Rana esculenta*. In addition to inhibiting the current, CN and ouabain depressed the plateaus but did not significantly change the amiloride corner frequency, except when ouabain was used in the presence of basolateral potassium and amphotericin B. The change in frequency in this case was rather negligible. In a symposium on lithium, Li and Lindemann [33] report one experiment on *R. ridibunda* skins in which ouabain inhibition in the presence of basolateral potassium did not alter the amiloride corner frequency. Van Driessche and Erlij [23] reported that in 18 *R. catesbeiana* skins the amiloride on-rate constant was significantly depressed from 18.8 ± 0.7 in the control to $14.4 \pm 1.0\ \mu M^{-1} \cdot s^{-1}$ for inward sodium current after ouabain and to $15.2 \pm 0.6\ \mu M^{-1} \cdot s^{-1}$ for outward sodium current. The off-rate constants were not significantly different. Although 18 skins were used, a variable number of determinations were reported at each amiloride concentration. The experiments were carried out with basolateral potassium replacing all sodium. The discrepancy with the present result that f_c is unchanged may be due to the species, since the sodium effect has not been reported in the bullfrog. Taken together, these findings show that the inhibition of the amiloride association rate by increased apical sodium concentration is not attributable to increased intracellular sodium.

Our third conclusion is that the apical sodium effect is not an indirect effect of a change in potential across the apical membrane. The electric field is not the determining factor in the competition between sodium and amiloride. Our experimental results support the original hypothesis [4] that amiloride and apical sodium interact rather directly at the apical face of the epithelium. The experiments of Palmer [25,26] and of Warnke and Lindemann [27,28] also suggest a direct competition in toad bladder. However, it should be noted that in their experiments, the competition of amiloride (as well as various cations) with sodium was uncovered using large potential gradients in skins bathed in high basolateral potassium. Their experiments assume that even under high voltage gradients, no amiloride-inhibitable current is forced through the paracellular pathway [34]. The resistance of these pathways is thought to be controlled by the zonulae occludentia, a structure which can be osmotically disrupted with solutes as large as raffinose [35,36]. The junctional structure appears to act as a non-selective diffusional barrier. It consists of lines of tightly packed fibrils at the interface joining contiguous granular cells [37,38]. The high concentrations of amiloride used to block the apical sodium-selective channels in order to determine the residual leakage current via such tight junctions may also block paracellular leakage current [14]. Furthermore, the paracellular pathway seems to affect the changes in transcellular resistance during hyperpolarizing pulses [39]. The interpretation of large currents overdriven by large polarizing pulses is not at all clear. Thus, that type of field-induced competition hypothesized from such experiments may or may not involve the same mechanism as the sodium effect reported here. Non-specific blocking actions, being diffusional in nature, seem unlikely to give rise to current fluctuations of the type seen with sodium-selective apical channels.

Concerning the mechanism by which basolateral potassium abolishes the sodium effect, Lindemann and Warncke [40] suggest that the original failure to observe the sodium effect was due to their use of potassium to substitute for apical sodium. They state that both sodium and potassium compete with amiloride and that in the 1979 experiments [5] the sum of the two cations was kept constant in the apical solution. However, we found previously that the sodium effect was present regardless of the replacement cation, or whether apical sodium was replaced with mannitol [2]. It is possible that a decreased intracellular pH may cause an increased affinity of the amiloride site. Civan and Peterson-Yantorno [41] reported in

TABLE IV

CALCULATED emf VALUES, CONDUCTANCES, CHANNEL DENSITIES AND SINGLE-CHANNEL CURRENTS

Experiment	n	E (mV)	g_o ($mS \cdot cm^{-2}$)	g_s ($mS \cdot cm^{-2}$)	N (μm^{-2})	i (pA)
$[Na]_i = 115$ mM	9	82 ± 9	0.064 ± 0.011	0.13 ± 0.02	3.5 ± 0.9	0.23 ± 0.23
$[Na]_i = 115$ mM, amphotericin B	4	98 ± 24	0.074 ± 0.011	0.17 ± 0.06	6.0 ± 1.8	0.14 ± 0.01
$[Na]_i = 115$ mM,	3	30	-0.001	0.11	0.007	0.64
amphotericin B,		65	0.025	0.11	1.4	0.13
0.1 mM ouabain		18	-0.006	0.14	1.4	0.06
$[K^+]_i = 120$ mM	4	42 ± 4	0.080 ± 0.036	0.21 ± 0.05	2.6 ± 0.9	0.22 ± 0.07
$[K]_i = 120$ mM, amphotericin B	11	44 ± 4	0.015 ± 0.052	0.42 ± 0.13	6.4 ± 0.13	0.24 ± 0.07
$[K]_i = 120$ mM,	3	52	0.102	0.075	3.4	0.17
amphotericin B,		58	0.014	0.26	0.6	0.14
5 mM CN		26	0.086	0.19	2.5	0.10
$[K]_i = 120$ mM, amphotericin B, 0.1 mM ouabain	4	22 ± 4	0.20 ± 0.10	0.95 ± 0.67	37.0 ± 29.0	0.22 ± 0.18

abstract that low apical sodium concentration resulted in a decrease in intracellular pH in *R. pipiens* skin. Basolateral potassium may stabilize intracellular pH and thereby prevent the effect of low apical sodium concentration. The same abstract states that vasopressin also decreased intracellular pH. However, Li et al. [42] had reported previously that vasopressin had no effect on the amiloride corner frequency in toad bladder. Clearly, new approaches are necessary to answer this question.

The present results confirm and extend the previously reported relation between noise and current [15]. This constitutes experimental support for the theory that the single-channel current pulses that sum up to give the short-circuit current are also in fact the same single-channel current pulses responsible for the fluctuations that give rise to noise power. In addition, knowledge of the voltage dependence of amiloride noise permitted estimation of paracellular and cellular pathway conductances simultaneously at low blocker concentrations, avoiding the need to (a) measure current at high amiloride concentration and (b) assume that the paracellular pathway is unaffected by high amiloride concentration. Hitherto it has not been possible to determine the magnitude of the shunt conductance without this latter assumption, an assumption which has not yet been fully justified (cf. Ref. 14). The results serve to confirm the predictions of the Ussing two-pathway model of frog skin as applied to noise measurements.

Having obtained estimates for the sodium channel current, channel density and single-channel current could be calculated (see Appendix). The latter calculation (Eqns. A-4, A-6) is rather insensitive to the amiloride inhibition constant K_A at amiloride concentrations much higher than K_A, assumed to be 0.2 μM. The channel density calculation, on the other hand, depends sensitively on the very imperfectly known K_A value and on details of the kinetic model. Computed values of single-channel current and channel density are given in Table IV. As these studies were not planned with this calculation in mind, number of pieces of skin for any given experimental treatment was small. The uncertainty of the estimates is large; nevertheless, the control values are not unreasonable.

We conclude that our original suggestion that apical sodium competes kinetically with amiloride is supported. This conclusion, coupled with the high specificity of amiloride, implies that the amiloride inhibition site may well be located close to the sodium-selective site. Moreover, the insensitivity of amiloride corner frequency to changes in clamp voltage means that the amiloride site is rather superficial [25–28] and not deep within the sodium channel, perhaps at the channel mouth itself.

Appendix

Using the noise power (low-frequency plateau value S_o) to find circuit parameters

The three circuit parameters are those of the model due to Ussing and Zerahn [16]:

g_o = conductance of transcellular pathway

g_s = shunt conductance (paracellular pathway)

E = membrane emf in series with g_o

The current-voltage relation (linear!) is

$$I = g_o E + (g_o + g_s)V$$

$$= I_o + g_s V$$

where I_o is the sodium-channel current.

In the past, separating out shunt conductance from channel conductance involved using sufficient blocker concentration to block g_o completely. With the Ussing model, a straight-line fit to the I-V relation has slope $(g_o + g_s)$ and current intercept $g_o E$. Indeed, a straight line has only two parameters. Repeating the measurements at high amiloride concentration and assuming all sodium channels blocked ($I_o = 0$) gives g_s separately, so that all three parameters are evaluated. The assumption of that classical procedure is that g_o is completely blocked and g_s is unaffected by high amiloride concentrations. Conceptually, the transcellular and paracellular pathways are distinguished by completely blocking the former. In the present approach, the transcellular current is distinguished as current component that exhibits amiloride noise. Now the assumption is that amiloride at moderate concentrations does not induce fluctuations in the paracellular current. Now, noise-power data give values of the two conductance parameters with the two assumptions that amiloride blocks g_o completely and leaves g_s unaffected.

For a 2-state model (channel open/channel blocked by amiloride), the low-frequency plateau value is *

$$S_o = \frac{4N}{k_-} \frac{[A]/K_A}{(1+[A]/K_A)^3} i^2 = ki^2 \qquad \text{(A-1)}$$

Here i is the single-channel current, and k_- is the amiloride dissociation rate constant; the second equation defines a proportionality constant k for given amiloride concentration [A]. The inhibition constant K_A is the amiloride concentration at which 50% of the sodium channels are blocked, making $(1 + [A]/K_A)^{-1}$ the fraction of channels open, so that, with N channels, we have

$$I_o = \frac{Ni}{(1+[A]/K_A)} = \frac{1}{c} i \qquad \text{(A-2)}$$

The assumption is implicit that amiloride-induced noise arises only at the apical, sodium-selective channels. This means that the shunt current $g_s V$ does not contribute to the observed noise, and that the plateau value of the Lorentzian noise spectrum is sufficiently greater than both the Johnson noise (which is independent of i) and the shot noise (which is proportional to i) that these may be neglected next to i^2 noise.

The formula for the corner frequency f_c of the Lorentzian fluctuation spectrum in terms of the 'off' rate constant k_-,

$$2\pi f_c = k_- (1+[A]/K_A) \qquad \text{(A-3)}$$

follows from the same 2-state model. Combining the three equations yields

$$i = \frac{S_o 2\pi f_c}{4 I_o} \left(1 + \frac{K_A}{[A]}\right) \qquad \text{(A-4)}$$

for the single-channel current. This is particularly useful at high blocker concentrations [A], where it gives a value of i rather insensitive to the inhibition constant K_A.

Our 3-state model [4] gives more complicated formulas in place of Eqns. A-1, A-2, and A-3, because it takes account of sodium-blocker competition. However, it gives the same asymptotic (i.e. high-blocker) form of Eqn. A-4 for the single-channel current.

Using the amiloride-dependent k and c defined in Eqns. A-1 and A-2, we write the plateau noise power S_o as

$$S_o = ki^2 = kc^2 I_o^2 \qquad \text{(A-5)}$$

Or, using the linear I-V relation, we can write it in

* The factor 4 in Eqn. A-1 becomes $1/\pi$ if frequency f is replaced by angular frequency $\omega = 2\pi f$ (see Eqn. 22 of Ref. 4). With this replacement, the convention is to integrate over negative frequencies as well as positive, hence the extra factor 2. For details, see Machlup [43].

terms of voltage only:

$$S_o = kc^2(I - g_s V)^2$$

$$= kc^2 g_o^2 (E + V)^2$$

$$= kc^2 g_o^2 (E^2 + 2EV + V^2)$$

That interprets the three A_i coefficients (S_o a quadratic in V) in terms of the model parameters as follows:

$$A_0 = kc^2 g_o^2 E^2,\ A_1 = 2kc^2 g_o^2 E,\ A_2 = kc^2 g_o^2$$

Rewriting S_o in terms of current only, we have

$$S_o = kc^2 g_o^2 \left(E + \frac{I - g_o E}{g_o + g_s} \right)^2$$

which interprets the three B_i coefficients in terms of the model parameters as follows:

$$B_0 = kc^2 \left(\frac{E}{1/g_o + 1/g_s} \right)^2, \quad B_1 = 2kc^2 \frac{E/g_s}{(1/g_o + 1/g_s)^2}$$

$$B_2 = kc^2 \frac{1}{(1/g_o + 1/g_s)^2}$$

Fitting parabolic curves first to the S_o-V relation and then to the S_o-I relation are logically equivalent procedures, since I and V are linearly related. Nonetheless, the A_i and B_i coefficients are then treated as though they were six independent empirical numbers. Various ratios of the six coefficients give values for the three circuit parameters. Putting in the three values, each of the six A and B coefficients gives an "independent" estimate of kc^2. Eqn. A-5 allows writing Eqn. A-4 in terms of kc^2:

$$i = \frac{2\pi f_c kc^2 I_o}{4} \left(1 + \frac{K_A}{[A]} \right) \qquad \text{(A-6)}$$

This equation can be used even without a good estimate of K_A because the ratio $K_A/[A]$ is so small. Had we used a blocker with a high dissociation rate k_-, the $K_A/[A]$ ratio would not have been small (i.e. much less than 1) in the measurable range of corner frequencies. In our experiments the ratio was about 0.1. Putting that value into Eqn. A-2 gives N, the number of sodium channels that give rise to I_o.

Acknowledgements

This work was supported in part by a grant from the United States Public Health Service No. AM5865.

References

1 Hoshiko, T. and Van Driessche, W. (1981) Arch. Int. Physiol. Biochim. 89, 58–60.
2 Hoshiko, T. and Van Driessche, W. (1986) J. Gen. Physiol. 87, 425–442.
3 Lindemann, B. and Van Driessche, W. (1978) in Membrane Transport Processes (Hoffman, J.F., ed.), pp. 155–178, Raven Press, New York, NY.
4 Frehland, E., Hoshiko, T. and Machlup, S. (1983) Biochim. Biophys. Acta 732, 636–646.
5 Van Driessche, W. and Lindemann, B. (1979) Nature (London) 282, 519–520.
6 Van Driessche, W. and Gögelein, H (1980) J. Theor. Biol. 86, 629–648.
7 Lindemann, B. and DeFelice, L.J. (1981) in Ion Transport in Epithelia (Schultz, S.G., ed.), pp. 1–13, Raven Press, New York, NY.
8 Valenzeno, D.P.a nd Hoshiko, T. (1977) Biochim. Biophys. Acta 470, 273–289.
9 Shum, W.K. and Fanelli, G.M. (1978) Biochim. Biophys. Acta 512, 593–597.
10 Cuthbert, A.W. and Shum, W.K. (1977) Nature (London) 266, 468–469.
11 Lindemann, B. (1984) Annu. Rev. Physiol. 46, 497–515.
12 Nagel, W. (1977) J. Physiol. 269, 777–796.
13 Rick, R., Dörge, A., Von Arnim, E. and Thurau, K. (1978) J. Membr. Biol. 39, 313–331.
14 Balaban, R.S., Mandel, L.J. and Benos, D.J. (1979) J. Membr. Biol. 49, 363–390.
15 Hoshiko, T. (1984) Curr. Top. Membr. Transp. 20, 3–26.
16 Ussing, H.H. and Zerahn, K. (1951) Acta Physiol. Scand. 23, 110–127.
17 Koefoed-Johnsen, V. and Ussing, H.H. (1958) Acta Physiol. Scand. 42, 298–308.
18 Ussing, H.H. and Windhager, E.E. (1964) Acta Physiol. Scand. 61, 484–504.
19 Helman, S.I. and Miller, D.A. (1971) Science (Wash. DC) 173, 146–148.
20 Menninger, J.R., Snell, F.M. and Spangler, R.A. (1960) Rev. Sci. Instr. 31, 519–521.
21 Helman, S.I., Nagel, W. and Fisher, R.S. (1979) J. Gen. Physiol. 74, 105–127.
22 Van Driessche, W. and Zeiske, W. (1980) J. Membr. Biol. 56, 31–42.
23 Van Driessche, W. and Erlij, D. (1983) Pflügers Arch. 398, 179–188.

24 Bevington, P.R. (1969) Data Reduction and Error Analysis for the Physical Sciences, McGraw Hill, New York.
25 Palmer, L.G. (1984) J. Membr. Biol. 80, 153–165.
26 Palmer, L.G. (1985) J. Membr. Biol. 87, 191–199.
27 Warncke, J. and Lindemann, B. (1985) Pflügers Arch. 405(S1), S89–S94.
28 Warncke, J. and Lindemann, B. (1985) J. Membr. Biol. 86, 255–265.
29 Li, J.H.Y., Cragoe, E.J., Jr. and Lindemann, B. (1985) J. Membr. Biol. 83, 45–56.
30 Tang, J., Abramcheck, F.J., Van Driessche, W. and Helman, S.I. (1985) Am. J. Physiol. 249, C421–C429.
31 Palmer, L.G. (1984) in Current Topics in Membranes and Transport. V. 20 Molecular approaches to epithelial transport. (Wade, J.B. and Lewis, S.A., eds.), pp. 105–121, Academic Press, New York.
32 Hoshiko, T., Grossman, R.A. and Machlup, S. (1984) Biophys. J. 45, 304a.
33 Li, J.H.Y. and Lindemann, B. (1982) in Basic Mechanisms in the Action of Lithium (Emrich, H.M., Aldenhoff, J.B. and Lux, H.D., eds.), pp. 28–35, Excerpta Medica, Amsterdam.
34 Bobrycki, V.A., Mills, J.W., Macknight, A.D.C. and DiBona, D.R. (1981) J. Membr. Biol. 60, 21–33.
35 DiBona, D.R. (1972) Nature New Biol. 238, 179–181.
36 Bindslev, N., McD. Tormey, J., Pietras, R.J. and Wright, E.M. (1974) Biochim. Biophys. Acta 332, 286–297.
37 Wade, J.B. and Karnovsky, M.J. (1974) J. Cell Biol. 62, 344–350.
38 Møllgård, K. and Rostgaard, J. (1981) in Ion Transport by Epithelia (Schultz, S.G., ed.), pp. 209–231, Raven Press, New York.
39 Finn, A.L., Davis, C.W. and Narvarte, J. (1981) in Ion Transport by Epithelia (Schultz, S.G., ed.), pp. 61–78, Raven Press, New York.
40 Lindemann, B. and Warncke, J. (1985) Pflügers Arch. 403, R13.
41 Civan, M.M. and Peterson-Yantorno, K. (1987) Fed. Proc. 46, 1268.
42 Li, J.H.Y., Palmer, L.G., Edelman, I.S. and Lindemann, B. (1982) J. Membr. Biol. 64, 77–89.
43 Machlup, S. (1954) J. Applied Phys. 25, 341–343.
44 Hoshiko, T., Grossman, R.A. and Machlup, S. (1987) Biophys. J. 51, 343a.